

Fig. 2. (a) Equivalent circuit of the dipole antenna. (b) Equivalent RLC resonant circuit.

L_{a1} and L_{a2} are the equivalent inductances; R_{a1} and R_{a2} are the equivalent radiation resistances. Together with the on-chip capacitors, C_{O1} and C_{O2} , they form RLC resonant circuits, which resonate in the operating frequency to filter the second harmonic and above. Figure 2(b) shows the equivalent RLC resonant circuit. Assume that $L_{a1} = L_{a2} = L_a$ (R_a , C_O , L'_a and R'_a are the same), then:

$$R'_a = R_a(Q_{RLC}^2 + 1), \tag{1}$$

$$L'_a = L_a \frac{Q_{RLC}^2 + 1}{Q_{RLC}^2}. \tag{2}$$

Q_{RLC} represents the Q value of the resonant circuit.

$$Q_{RLC} = \frac{R'_a}{\sqrt{L'_a/C_O}}. \tag{3}$$

The maximum output power $P_{OUT_{max}}$ of the PA is determined as follows by load impedance R'_a and the supply voltage V_{DD} .

$$P_{OUT_{max}} = \frac{V_{DD}^2}{2R'_a} \times 2. \tag{4}$$

To work at 2.45 GHz and obtain an appropriate Q_{RLC} , the L_a of 5 nH is designed. The on-chip capacitance is 650 fF in consideration of parasitic capacitance. R_a is 26 Ω since the expected maximum total output power of the PA is 10 dBm with the supply voltage of 1.8 V.

A differential structure and a cascode configuration have been used in the design. Due to the symmetry of the differential structure, the noise coupling through the power supply and ground connections to chips can be suppressed effectively. Also, a differential structure can reduce the sensitivity of the power amplifier to package parasitics.

According to Ref. [4], oxide breakdown is a serious issue in the design of power amplifiers in submicron CMOS. A cascode topology is chosen to improve output voltage swing of

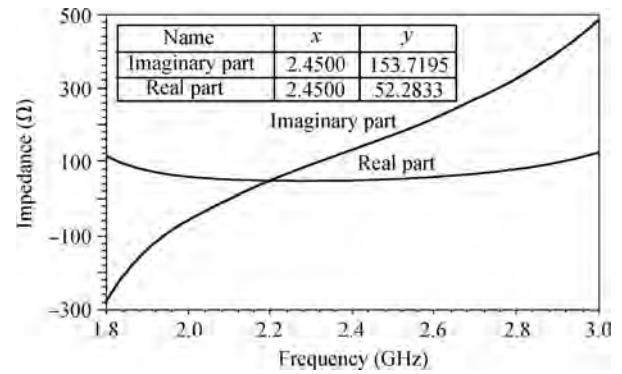


Fig. 3. Dipole antenna impedance.

the power amplifier. As shown in Fig. 1, transistors M1–M2 act as a common source (CS) and transistors M3–M4 act as a common gate (CG). The differential RF signal is applied to V_{in+} and V_{in-} . The gates of M3 and M4 are RF grounded with supply voltage V_{DD} . The maximum voltage that CG transistors can withstand is $V_{DGC(MAX)}$.

$$V_{DGC(MAX)} = V_{OUT(MAX)} - V_{DD}. \tag{5}$$

$V_{OUT(MAX)}$ is the maximum output voltage of PA. The voltage that CS transistors are able to withstand is V_{DGS} .

$$V_{DGS} = V_{CASC} - V_{IN}. \tag{6}$$

V_{CASC} is the source voltage of the CG transistors. V_{IN} is the input voltage. V_{CASC} increases as V_{IN} decreases. When V_{CASC} increases to $V_{DD} - V_T$, the CG transistors are off. So the maximum voltage that CS transistors can withstand is $V_{DGS(MAX)}$.

$$V_{DGS(MAX)} = V_{DD} - V_T - V_{IN(MIN)}. \tag{7}$$

Usually, $V_{DGS(MAX)}$ is less than the gate oxide breakdown voltage ($> 2V_{DD}$) of the transistor. To prevent the transistors from breakdown,

$$V_{DGC(MAX)} = V_{DD} + 2V_{DD} = 3V_{DD}. \tag{8}$$

So the maximum output voltage is $3V_{DD}$ after using the cascode topology. While the maximum output voltage is only $2V_{DD} + V_{IN(MIN)}$ without the use of the cascode topology. $V_{IN(MIN)}$ is close to 0 or even negative.

3. Simulation and measurement results

Simulations and measurements were performed to find the antenna impedance, 1 dB compression point and spectral characteristic. The simulations were performed with Ansoft HFSS, Cadence, and the measurements with an Agilent-frequency spectrograph.

Figure 3 shows the dipole antenna impedance. The figure reveals that the real part is about 52 Ω and the imaginary part is 154 Ω , which means R_a is 26 Ω and L_a is 5 nH.

The chip was fabricated in a 0.18 μm single poly 6-metal layer (1P6M) CMOS process. A microphotograph of the PA is shown in Fig. 4. The total chip area excluding the bonding wire pads is just $240 \times 70 \mu\text{m}^2$.

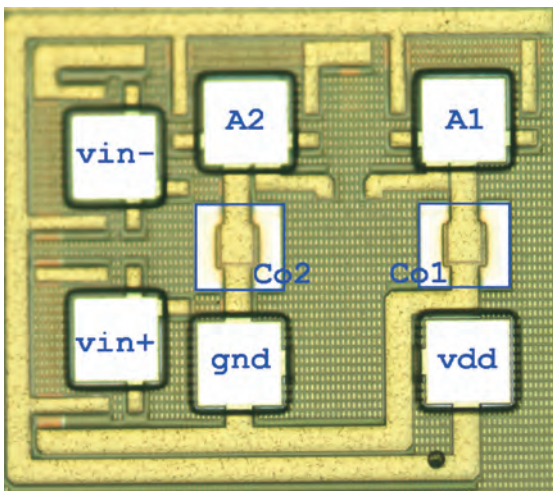


Fig. 4. Die photo of power amplifier.

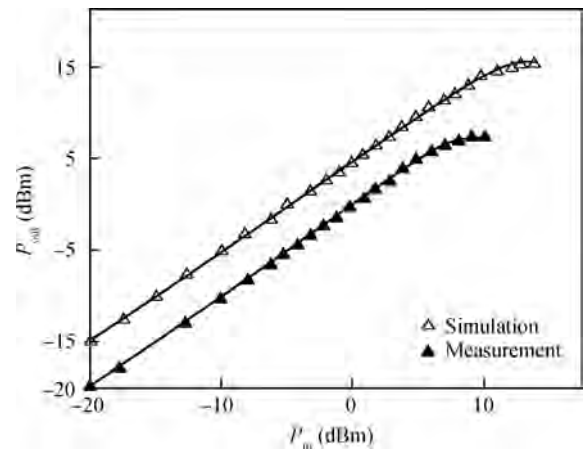


Fig. 6. Measured and simulated output power at 2.45 GHz.

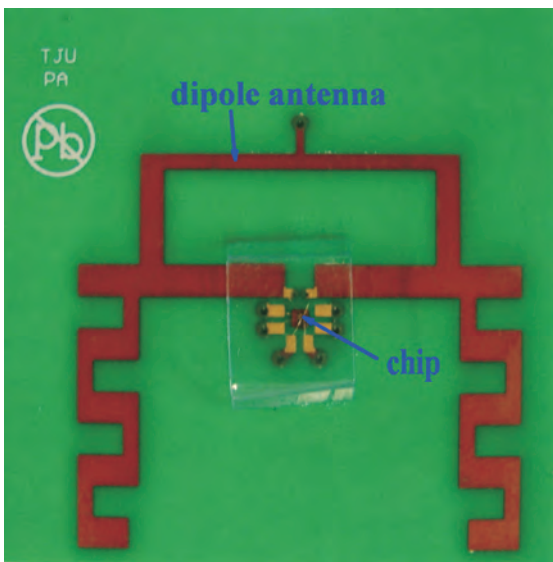


Fig. 5. One side of the PCB.

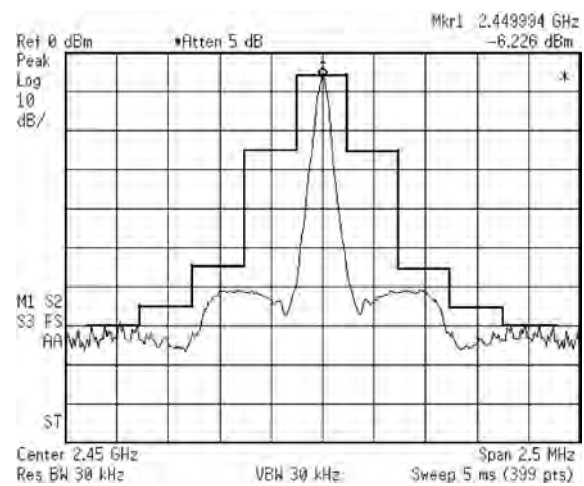


Fig. 7. Measured output spectrum and spectral mask for a multiple reader environment.

The chip was glued directly onto the PCB board using an electrically and thermally conductive adhesive. The pads were wire bonded to the gold-plated metal lines on the PCB. As shown in Fig. 5, the bare copper strip is the designed dipole antenna. An input balun transformer is appended to the circuit to generate differential input signals. To reduce the impact on antenna impedance, balun and copper traces are placed on the other side of the PCB.

The measured output power of the PA is shown in Fig. 6. The frequency of the input signal generated by the network analyzer is 2.45 GHz. The output signals are received by an Agilent E4402B frequency spectrograph. With a supply voltage of 1.8 V and gate bias voltages of 0.6 V, the PA provides an output P_{1dB} of 8 dBm. The post layout simulated results are also illustrated in Fig. 6. The difference between the measured and simulated power is 5 dBm, which results from the insufficient accuracy of the RF transistor models and transmission loss. The simulation results do not take process deviation into account. The characteristic impedance of the spectrum analyzer probe is 50 Ω , but output impedance matching network for test is not

designed, which increases the power loss. This also leads to bad power added efficiency (PAE). So the measured PAE is not shown in Fig. 6. Further work is needed to improve measured characteristic.

Other important characteristics of a PA are the transmitted spectral requirements. A single carrier signal is applied to the PA. The measured result shows that the spectrum at the PA output satisfies the require spectrum mask in the multiple-reader environment condition of the EPC global Class 1 Generation 2 standard.

4. Conclusion

In this paper, a novel power amplifier design has been proposed. Associated with the design of PCB antenna, on-chip RF integrated inductors are not applied. The outputs of the PA are directly applied to a symmetrical dipole antenna with a differential structure. Based on this technique, a new matching method between the PA and antenna of an active or semi-active RFID tag is established. The total chip area is also reduced greatly to only 240 \times 70 μm^2 . The function of the PA is verified with 0.18 μm 1P6M CMOS process. Measurements show that the PA can provide an output power of 8 dBm at the 1 dB

compression point. Finally, the spectrum is tested for the specified EPC global Class 1 Generation 2 Standard Protocol.

References

- [1] Kim S, Cho J H, Kim H S, et al. An EPC Gen 2 compatible passive/semi-active UHF RFID transponder with embedded FeRAM and temperature sensor. IEEE Asian Solid-State Circuits Conference, A-SSCC, Jeju, Korea, 2007
- [2] Aluf O. Active RFID TAGs system analysis of energy consumption as excitable linear bifurcation system. IEEE International Conference on Microwaves, Communications, Antennas and Electronics Systems, 2009
- [3] Qian Y B, Li W Y, Wang Z G. 2.4-GHz 0.18- μm CMOS highly linear power amplifier. International Conference on Advanced Technologies for Communications, 2010
- [4] Sowlati T, Leenaerts D M W. A 2.4-GHz 0.18- μm CMOS self-biased cascode power amplifier. IEEE J Solid-State Circuits, 2003, 38(8): 1318
- [5] Sowlati T, Leenaerts D. A 2.4 GHz 0.18 μm CMOS self-biased cascode power amplifier with 23 dBm output power. IEEE International Solid-State Circuits Conference, Digest of Technical Papers, 2002
- [6] Jian F, Shilei H, Yumei H, et al. A 2.4 GHz CMOS power amplifier. 10th IEEE International Conference on Solid-State and Integrated Circuit Technology, 2010
- [7] Kocer F, Flynn M P. A new transponder architecture for long-range telemetry applications. Proceedings of the European Conference on Circuit Theory and Design, 2005
- [8] EPC Radio-Frequency Identity Protocols. Class-1 generation-2 UHF RFID, protocol for communications at 860 MHz–960 MHz. Version 1.0.9, Jan 31, 2005
- [9] Cho C, Choo H, Park I. Printed symmetric inverted-f antenna with a quasi-isotropic radiation pattern. Microwave and Optical Technology Letters, 2008, 50(4): 927